Catalysis Today 165 (2011) 56–63

Contents lists available at ScienceDirect

Catalysis Today

journal homepage: www.elsevier.com/locate/cattod

Effects of heat and mass transfer on the kinetics of CO oxidation over $RuO_2(1\,1\,0)$ catalyst

Donghai Mei[a,*], Guang Lin[b]

[a] Institute for Interfacial Catalysis, Pacific Northwest National Laboratory, P.O. Box 999, Richland, WA 99352, USA
[b] Computational Science and Mathematics Division, Pacific Northwest National Laboratory, Richland, WA 99352, USA

ARTICLE INFO

Article history:
Received 15 September 2010
Received in revised form
17 November 2010
Accepted 17 November 2010
Available online 18 December 2010

Keywords:
Multiscale model
Heat and mass transfer
CO oxidation
First-principles kinetic Monte Carlo

ABSTRACT

Combining first-principles kinetic Monte Carlo (KMC) simulation with a finite difference continuum model, a hybrid computational model was developed to study the effects of heat and mass transfer on the heterogeneous reaction kinetics. The integrated computational framework consists of a surface phase where catalytic surface reactions occur and a gas-phase boundary layer imposed on the catalyst surface where the fluctuating temperature and pressure gradients exist. The surface phase domain is modeled by the site-explicit first-principles KMC simulation. The gas-phase boundary layer domain is described using the second-order grid-based Crank–Nicolson method. To simplify the model, the flow and gas-phase reactions are excluded. The temperature and pressure gradients in the gas-phase boundary layer are the consequence of thermal and molecular diffusions of reactants and products under nominal reaction conditions. Different from previous hybrid multiscale models, the heat and mass fluxes between two domains are directly coupled by the varying boundary conditions at each simulation timestep from the unsteady state reaction regime to the steady state reaction regime in the present model. At the steady-state reaction regime, the activity, the surface coverages of reaction intermediates, along with the temperature and pressure gradient profiles in the gas-phase boundary layer are statistically constant with very small fluctuations. As an illustration example, we studied the effects of heat and mass transfer on the reaction kinetics of CO oxidation over the $RuO_2(1\,1\,0)$ catalysts. We assume the heat from CO oxidation is exclusively dissipated into the gas-phase via thermal diffusion. By varying the thickness of $RuO_2(1\,1\,0)$ catalysts, the surface temperature changes correspondingly with the heat produced by occurring surface reactions, resulting in the pronounced temperature and pressure gradients in the gas-phase boundary layer. Our simulation results indicate that the limitation of heat and mass transfer in the surrounding environment over the catalyst could dramatically affect the observed macroscopic reaction kinetics under presumed operating reaction conditions. To fully elucidate the complex heterogeneous catalytic system, proper physical description of fluid phase that imposed on the catalyst and its effect on the surface kinetics should be integrated with current surface computational models.

1. Introduction

Computational modeling plays an increasingly important role in the characterization and understanding of a broad range of elementary chemical transformations relevant to heterogeneous catalytic processes. It remains, however, a formidable challenge to computational models with a predictive capability that describe complex heterogeneous processes involving the intrinsic reaction kinetics and transport of momentum, mass and heat [1,2]. The fluctuating temperature and pressure (or concentrations) gradients in the fluid phase over catalysts in either industrial reactors or small-scale laboratory reactive equipments give rise to the inhomogeneous nature that dramatically complicates the observed macroscopic reaction kinetics. To model chemical transformation processes in such complex heterogeneous environment thus requires a computational approach or framework that includes the transport of reactants, reaction intermediates, and products, the addition or removal of reaction heat along with the accurate surface reaction model on the solid catalyst. In the past decade, a number of multiscale hybrid models have been developed to meet this requirement. These hybrid multiscale models generally combined molecular-level surface reaction models for the catalysts phase and macroscopic continuum models for the fluid phase. A common bottom-up approach was adopted, i.e., passing the information of thermodynamic, kinetics and transport properties at atomic or discrete scale to the continuum scale. For example, Vlachos et al. developed a hierarchical reactor model that coupled coarse-grained kinetic Monte Carlo (KMC) simulation with computational fluid

* Corresponding author.
E-mail address: donghai.mei@pnl.gov (D. Mei).

0920-5861/$ – see front matter © 2010 Elsevier B.V. All rights reserved.
doi:10.1016/j.cattod.2010.11.041

dynamics (CFD) [3–6]. They have applied this multiscale model to study the macroscopic kinetics of various catalytic systems such as preferential CO oxidation, water–gas shift, and ammonia decomposition on metal catalysts in plug-flow type reactors [7–9]. Majumder and Broadbelt also proposed a multiscale model that combined KMC with a finite difference (FD) solver to study the steady-state reaction kinetics in a two-dimensional flow reactor [10]. In those multiscale models, the entire catalytic heterogeneous reaction system is decomposed into two domains: the catalyst surface phase and the flow fluid phase. The catalyst surface domain is described by molecular-level microscopic kinetic models such as coarse-grained lattice KMC simulations. The thermodynamic and kinetic parameters database for elementary surface processes including adsorption, reaction, desorption and diffusion, which is required by KMC simulation as the input, are either obtained from experiments [10] or from first-principles density functional theory (DFT) calculations combined with unity bond index quadratic exponential potential (UBI-QEP) method [7,8,11,12]. For the fluid phase domain, a continuum model such as FD and CFD that describes the mass and heat transfer is used.

Very recently, Matera and Reuter proposed an multiscale computational model that integrates first-principles KMC simulations with a CFD solver for studying the effects of heat and mass transfer on the surface reaction kinetics of CO oxidation over $RuO_2(1\,1\,0)$ catalyst [13,14]. The fluid phase domain above the catalyst surface was modeled by a stagnant flow geometry that mimics the experimental surface science setup. They found that the limitations of heat and mass transfer significantly mask the measured CO oxidation kinetics. To avoid the possible instability of the algorithms used in the continuum model, Matera and Reuter decoupled the interdependence of first-principles KMC simulations with a continuum model [13,14]. In their approach, a series of first-principles KMC simulations were performed in a wide range of temperature and (partial) pressure conditions, to generate a grid map of catalytic activities at the steady-state conditions as the functions of temperatures and (partial) pressures. Those simulation data, which also included the data by interpolation, then provided the continuum model as the boundary conditions. In such a way, the averaged thermodynamic and kinetic variables at the steady-state conditions obtained from KMC simulations are then communicated with the continuum model in an iterative feed-response mode. The fluctuations of thermodynamic and kinetics information from stochastic KMC simulations are not considered. Furthermore, the important information of the unsteady-state surface reaction, which may affect the ultimate steady-state intrinsic kinetics if the surrounding fluid phase conditions change correspondingly, is also not communicated with the fluid phase. Instead of truly coupling the surface and the fluid phase models, the multiscale heterogeneous reaction model proposed by Matera and Reuter is implemented in the separate mode. The variations of the surrounding reaction environment imposed on the catalyst are not taken into account in the *real-time* fashion. Only the averaged, steady-state KMC simulation results were used as the boundary conditions for the continuum models.

The methodology and the spirit proposed by Matera and Reuter actually intrigued the present work. Herein we propose a heterogeneous reaction model that directly couples first-principles KMC simulation with a finite difference continuum model in a real-time dynamical mode. The changes in the temperature and partial pressures obtained from heat and mass transfer in gas phase are taken into account before the steady-state reaction condition for the entire catalytic system is reached. At each time step, the surface temperature and the concentrations (or partial pressures) of reactants and products obtained from KMC simulation are directly used as the *in situ* boundary conditions for the continuum model. The temperature and the concentrations of the nearest adjacent gas phase layer, that are obtained from the continuum model simulation are used as the *in situ* reaction condition for KMC simulation in the next time step. As such, our proposed reaction model captures the inhomogeneous dynamical nature in both the gas phase and the surface phase domains simultaneously. CO oxidation on $RuO_2(1\,1\,0)$ catalyst has been well studied both experimentally and theoretically [12,13,15–20]. To compare with the results of Matera and Reuter [13,14], we choose the same reaction system, as the benchmark reaction system to demonstrate the proposed model. For simplicity, the heat and mass transfer in the stagnant boundary layer above the $RuO_2(1\,1\,0)$ catalyst surface are only described by thermal and molecular diffusions. Since CO oxidation on the $RuO_2(1\,1\,0)$ catalyst is exothermic, the degree of increase for the surface temperature caused by CO oxidation occurring on the surface varies with the thickness of the catalyst. The variations of the surface temperature corresponding to different catalyst thicknesses eventually affect the intrinsic surface kinetics even though the nominal invariant operating conditions that set in the bulk fluid phase are the same. In this work, we focus on the effect of the catalyst thickness on the intrinsic reaction kinetics of CO oxidation on the $RuO_2(1\,1\,0)$ catalyst.

2. Methodology

Similar to the previous multiscale models [5,10], the entire heterogeneous catalytic reaction system is decomposed into the catalyst surface phase domain and the stagnant gas-phase boundary layer domain. As shown in Fig. 1, the nominal operating reaction condition such as the temperature ($T^{(n)}$) and the partial pressures $\left(P_{CO}^{(n)} \text{ and } P_{O_2}^{(n)}\right)$ beyond the boundary layer are constant. The gas-phase boundary layer is assumed as the stagnant gas phase without bulk flow. Only the molecular diffusions of reactants (CO and O_2) and the product (CO_2) are considered (mass transfer). The heat transfer in the boundary layer is described as the thermal diffusion process. The first-principles KMC simulation and second-order Crank–Nicolson method are used for the surface phase and the gas-phase boundary layer domains, respectively.

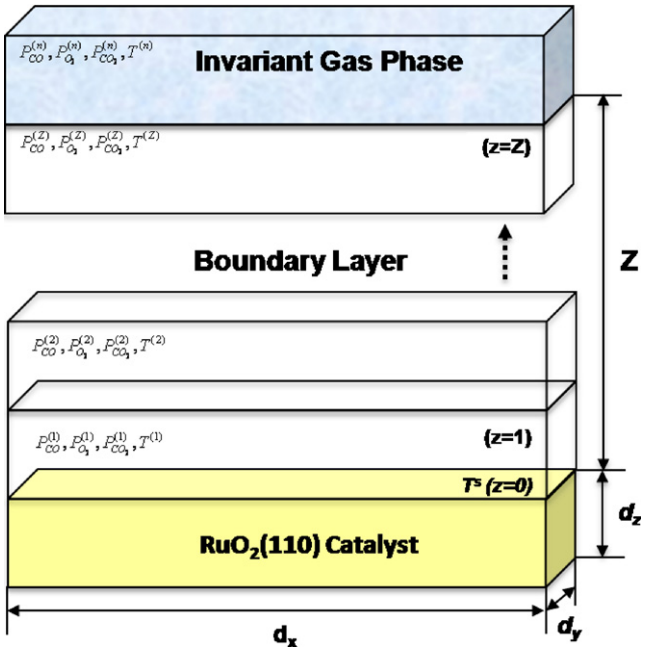

Fig. 1. Schematic diagram of the multiscale model.

2.1. Kinetic Monte Carlo simulation

The surface phase domain consists of the rutile $RuO_2(1\,1\,0)$ catalyst with a surface grid size of $(d_x \times d_y)$ and the various thicknesses. The thickness of the $RuO_2(1\,1\,0)$ catalyst is represented by the number of layers (d_z). Each surface site ($d_x \times d_y = 1 \times 1$) with a surface area of $A_s = 10.03\,\text{Å}^2$ consists of one cus site and one bridge site on the $RuO_2(1\,1\,0)$ surface. CO and O_2 molecules adsorb on both cus and bridge sites. As indicated in the previous first-principles KMC simulation study [12], the unsaturated cus and bridge sites are active for CO oxidation. Adsorbed CO* reacts with the neighboring atomic surface oxygen (O*) that formed by O_2 dissociative adsorption produce CO_2 that directly release into the adjacent gas-phase layer above the catalyst surface. A total of 26 elementary surface processes such as adsorptions and desorptions of CO, O_2 and CO_2, CO oxidation at different surface sites, and surface diffusions of CO* and O* are included in the first-principles KMC simulation. Please note that CO_2 re-adsorption is not considered in the KMC simulations. The periodic boundary conditions in x and y directions are applied in the KMC simulations. To avoid the artifact of the surface size effect on the reaction kinetics, a series of surface grid sizes ranging from $(d_x \times d_y = 40 \times 40)$ to $(d_x \times d_y = 200 \times 200)$ were tested. The surface grid size of $(d_x \times d_y = 100 \times 100)$ is found to be statistically accurate enough. A site-explicit variable time-step algorithm [21–26] is used in the KMC simulations. Based on the normalized probabilities of the occurring surface processes, only one surface process of 26 elementary processes occurs at each KMC simulation time step (Δt). The normalized probability of each surface process is determined by the reaction rates of all elementary surface processes that are calculated using first-principles DFT data reported by Reuter and Scheffler [12,27]. The details of the reaction rate calculations, which can be found in the previous publication [12], are not repeated here.

2.2. Continuum model

Practically, various thicknesses or layers of the well-defined $RuO_2(1\,1\,0)$ surface slabs correspond to different sizes of the RuO_2 catalysts. If the RuO_2 catalyst is very good thermal conductor material, the heat released by CO oxidation occurring on the surface would rapidly dissipate into the whole catalyst without local "hot" spot. The degree of variation of the surface temperature, which is the same as the catalyst temperature, is determined by the catalyst size and the exchange rate with the surrounding environment. As CO oxidation occurs from the time step t to $t+\Delta t$, the surface temperature $T^{(s)}(t+\Delta t)$ at the time step $t+\Delta t$ becomes:

$$T^{(s)}(t+\Delta t) = T^{(s)}(t) + \frac{\Delta H}{C_p \cdot \rho_c \cdot V_c} \tag{1}$$

here ΔH is the reaction enthalpy of CO oxidation; C_p ($= 25.0\,\text{J mol}^{-1}\,\text{K}^{-1}$) and ρ_c ($= 6.97\,\text{g mol}^{-1}$) are the heat capacity and the density of $RuO_2(1\,1\,0)$ catalyst, respectively. V_c ($= d_x \times d_y \times d_z \times A_s$) is the volume of $RuO_2(1\,1\,0)$ catalyst. So the variation of surface temperature $T^{(s)}$ is determined by the thickness of the $RuO_2(1\,1\,0)$ catalyst (d_z). A smaller perturbation of the surface temperature occurring on the larger catalyst particles is expected. Furthermore, as the catalytic surface reaction progresses, the catalyst surface temperature is actually different from the nominal operating temperature measured in bulk gas-phase which is constant. Therefore, a temperature gradient is formed in the gas-phase boundary layer between the catalyst surface and the bulk gas-phase. The *in situ* surface temperature then is affected by the heat transfer that is described by the thermal diffusion in the boundary layer.

To sustain the steady catalytic surface reactions, on the other hand, all the reactant molecules must continuously move to the adjacent gas-phase region above the catalyst surface and readily adsorb on the surface. At the same time, the product molecule that desorbs into the adjacent gas-phase region have to be moved away from the catalyst surface to avoid the re-adsorption. If the gas-phase boundary layer is stagnant, only molecular diffusion is accounted for mass transfer. Obviously, there must be the pressure gradients for reactants and products in the stagnant boundary layer between the bulk gas-phase and the catalysts surface. As such, there are both temperature and pressure gradients in the gas-phase boundary layer.

Table 1
Diffusion coefficients of CO, O_2 and CO_2 used in the continuum model.

D_{CO}	$6.43 \times 10^{-9}\,\text{m}^2\,\text{s}^{-1}$
D_{O_2}	$3.84 \times 10^{-9}\,\text{m}^2\,\text{s}^{-1}$
D_{CO_2}	$5.35 \times 10^{-9}\,\text{m}^2\,\text{s}^{-1}$

The heat and mass transfer in the gas-phase boundary layer can be described by the molecular diffusion and thermal diffusion. In this work, the gas-phase boundary layer domain is characterized using regular cubic mesh grids. The boundary layer thickness (Z) is 1.0×10^{-3} mm. The boundary layer is divided to ten equally spaced grids ($d_{gz} = Z/10$) in z direction. To match the size of the surface grid, the periodic grid ($d_x \times d_y = 100 \times 100$) is also used in x and y directions of the boundary layer. The gas-phase grid boundary layer domain consists of $100 \times 100 \times 10$ mesh points.

To further simplify the continuum model, the gas-phase boundary layer is treated as the ideal gas mixtures without gas-phase reactions. We also assume there is no heat transfer being removed from the backside of the $RuO_2(1\,1\,0)$ catalyst. On the basis of these two assumptions, the concentrations of reactive species and the temperature at each gas-phase grid point along the z direction can be obtained as follows:

$$\frac{\partial C_i(T^{(z)}, z, t)}{\partial t} = D_i \frac{\partial^2 C_i(T^{(z)}, z, t)}{\partial^2 z} \tag{2}$$

$$\frac{\partial T^{(z)}(z, t)}{\partial t} = \lambda_z \frac{\partial^2 T^{(z)}(z, t)}{\partial^2 z} \tag{3}$$

$$C_i(T^{(z)}, z, t) = \frac{N_i(T^{(z)}, z, t)}{V_g} = \frac{P_i(T^{(z)}, z, t)}{RT^{(z)}} \tag{4}$$

where $C_i(T^{(z)}, z, t)$ is the concentration of species i (i = CO, O_2 and CO_2) in the gas-phase grid z at time t. $P_i(T^{(z)}, z, t)$ and $N_i(T^{(z)}, z, t)$ are the partial pressure and the total number of species i in the gas-phase grid z at time t, respectively. V_g is the volume of each gas-phase grid ($V_g = d_x \times d_y \times A_s \times d_{gz}$). $T^{(z)}$ is the temperature in the gas-phase grid z. D_i is the diffusion coefficient of species i. Table 1 lists the diffusion coefficients of CO, O_2 and CO_2 used in this work. λ_z ($= 3.79 \times 10^{-2}\,\text{W m}^{-1}\,\text{K}^{-1}$) is the thermal conductivity coefficient of the gas phase mixtures.

Crank–Nicolson method is usually applied to diffusion problem in homogeneous systems for its unconditional stability [28]. Crank–Nicolson method is based on central difference in space and second-order in time. In this work, we use Crank–Nicolson method to solve the master equations for heat and mass transfer in the gas-phase boundary layer (Eqs. (2) and (3)). For example, the one-dimension molecular diffusion in z direction can be implicitly solved using:

$$\frac{C_i(T^{(z)}, z, t+\Delta t) - C_i(T^{(z)}, z, t)}{\Delta t} = \frac{D_i}{2d_{gz}^2}\left[{F_c}^{t+\Delta t} + {F_c}^{t}\right] \tag{5}$$

in which

$${F_c}^{t+\Delta t} = C_i(T^{(z)}, z+\Delta z, t+\Delta t) - 2C_i(T^{(z)}, z, t+\Delta t) + C_i(T^{(z)}, z-\Delta z, t+\Delta t) \tag{6}$$

$$F_c{}^t = C_i(T^{(z)}, z+\Delta z, t) - 2C_i(T^{(z)}, z, t) + C_i(T^{(z)}, z-\Delta z, t) \quad (7)$$

Similarly, the temperature gradient profile in the gas-phase boundary layer can be described as

$$\frac{T^{(z)}(z, t+\Delta t) - T^{(z)}(z, t)}{\Delta t} = \frac{\lambda_z}{2d_{gz}^2}\left[F_T{}^{t+\Delta t} + F_T{}^t\right] \quad (8)$$

$$F_T{}^{t+\Delta t} = T^{(z+\Delta z)}(z+\Delta z, t+\Delta t) - 2T^{(z)}(z, t+\Delta t) + T^{(z-\Delta z)}(z-\Delta z, t+\Delta t) \quad (9)$$

$$F_T{}^t = T^{(z+\Delta z)}(z+\Delta z, t) - 2T^{(z)}(z, t) + T^{(z-\Delta z)}(z-\Delta z, t) \quad (10)$$

2.3. Dynamical coupling

To obtain the pressure and temperature gradient profiles using Crank–Nicolson method, both upper- and lower-limit boundary conditions are needed. As shown in Fig. 1, the upper-limit boundary ($z = Z$) condition is the nominal operating reaction condition ($T^{(n)}$, $P_{CO}^{(n)}$ and $P_{O_2}^{(n)}$), which are constant values in the simulations. As the CO oxidation reaction occurs on the surface, CO_2 desorbs into the gas-phase boundary layer, and then diffuses to the gas-phase bulk. Therefore, there is also a pressure gradient of CO_2 formed in the gas-phase boundary layer. The partial pressure of CO_2 in the bulk gas-phase at the simulation step $t + \Delta t$ is the same as the outermost boundary layer $\left(P_{CO_2}^{(Z)}\right)$ at the simulation step t. The upper-limit boundary condition ($z = Z$) for the gas-phase boundary layer is given in Eq. (11):

$$\begin{aligned} P_{CO}^{(Z)}(t+\Delta t) &= P_{CO}^{(n)} \\ P_{O_2}^{(Z)}(t+\Delta t) &= P_{O_2}^{(n)} \\ P_{CO_2}^{(Z)}(t+\Delta t) &= P_{CO_2}^{(Z)}(t) \\ T^{(Z)}(t+\Delta t) &= T^{(n)} \end{aligned} \quad (11)$$

The treatment of the lower limit boundary condition is the key in coupling two physical models for different phase domains. In the previous multiscale heterogeneous–homogenous reaction models [5,10,13,29], the time-averaged output from the stochastic KMC simulation at the steady-state reaction condition was used as the lower-limit boundary condition for the continuum CFD model. The fluctuations of surface kinetics information from the stochastic KMC simulations are filtered to avoid the instability of CFD simulation [10]. This is largely because the small surface grid size was used. In the present model, the lower limit boundary condition is directly connected with KMC simulation output at each time step. The *real-time in situ* temperature and the partial pressures with fluctuations in the interfacial layer ($z = 1$) that is adjacent to the surface are used as the lower-limit boundary condition for Crank–Nicolson continuum model. At each simulation step t, the lower-limit boundary condition from the first-principles KMC simulation will be fed into the continuum model. The continuum model results of $P_i(T^{(1)}, z = 1, t)$ and $T^{(1)}(t)$ used as the *in situ* reaction condition for the KMC simulation in the next simulation step $t + \Delta t$.

The mass transfer is the consequence of the adsorptions and desorptions of reactants and the product. Because only one surface process is allowed to occur at each KMC simulation step, the total number N_i of each species i (i = CO, O_2 and CO_2) in the interfacial layer at simulation step $t + \Delta t$ is

$$N_i(t+\Delta t, z=1) = N_i(t, z=1) + \delta_i \quad \begin{array}{l} \delta_i = 1 \quad \text{if adsorption of species i occurs} \\ \delta_i = -1 \quad \text{if desorpiton of species i occurs} \end{array} \quad (12)$$

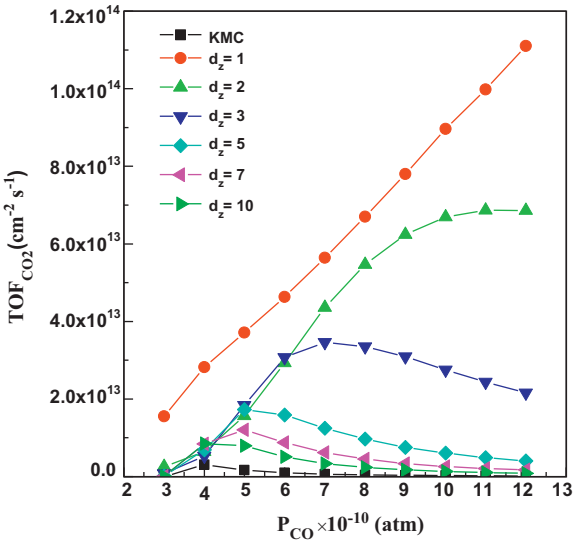

Fig. 2. Simulated CO_2 TOFs as a fucntion of $P_{CO}^{(n)}$ at the nominal reaction condition of $T^{(n)} = 350$ K and $P_{O_2}^{(n)} = 1.0 \times 10^{-10}$ atm.

Therefore, we obtain the lower limit boundary condition for Crank–Nicolson continuum model.

$$\begin{aligned} P_{CO}^{(1)}(t+\Delta t) &= \frac{N_{CO}^{(1)}(t+\Delta t)\cdot R\cdot T^{(1)}}{V_g} \\ P_{O_2}^{(1)}(t+\Delta t) &= \frac{N_{O_2}^{(1)}(t+\Delta t)\cdot R\cdot T^{(1)}}{V_g} \\ P_{CO_2}^{(1)}(t+\Delta t) &= \frac{N_{CO_2}^{(1)}(t+\Delta t)\cdot R\cdot T^{(1)}}{V_g} \\ T^{(1)}(t+\Delta t) &= T^{(s)}(t+\Delta t) \end{aligned} \quad (13)$$

3. Results and discussion

The reaction kinetics of CO oxidation over the $RuO_2(1\,1\,0)$ catalyst under invariant gas-phase reaction conditions had been investigated using first-principles KMC simulations [12,20,27]. To validate the KMC simulation model for the catalyst surface phase in the present model, we first performed first-principles KMC simulations of CO oxidation over the $RuO_2(1\,1\,0)$ surface under invariant gas-phase reaction conditions. The temperature and pressure gradients in the gas-phase as well as the surface temperature change induced by the exothermic CO oxidation are not considered. The surface temperature ($T^{(s)}$) is the same as the nominal temperature ($T^{(n)}$). And the surface temperature is not affected by the heat that is generated from exothermic CO oxidation. In other words, the reaction heat is being removed from the entire system very quickly. Similarly, the partial pressures in the adjacent gas-phase imposed on the catalyst surface ($P_{CO}^{(1)}$ and $P_{O_2}^{(1)}$) are the same as the nominal partial pressures ($P_{CO}^{(n)}$ and $P_{O_2}^{(n)}$). Under this ideal circumstance, the reaction kinetics obtained from first-principles KMC simulations is referred to the *intrinsic* reaction kinetics.

Fig. 2 shows the normalized turnover frequencies (TOFs) of CO_2 as a function of CO partial pressure at $T^{(n)} = 350$ K and $P_{O_2}^{(n)} = 1.0 \times 10^{-10}$ atm. The normalized TOF of CO_2 is the total number of CO_2 molecules that desorb from the surface per site per second. Our

simulation results suggest that the most active reaction condition with the maximum CO_2 TOF corresponds to $P_{CO}^{(n)} = 4.0 \times 10^{-10}$ atm. This is consistent with the previously reported KMC results [20]. The simulated CO_2 TOF is 3.63×10^{12} cm^{-2} s^{-1} which is also close to the reported value of 4.0×10^{12} cm^{-2} s^{-1} [20]. The small difference in absolute CO_2 TOF values is most likely due to the different surface grids used in this work and the KMC simulations by Temel et al. [20]. Our results also suggest that the activity of CO oxidation is very low in the low CO partial pressure range of $1.0–3.0 \times 10^{-10}$ atm. The simulated TOFs of CO_2 are several magnitude of orders smaller than the maximum CO_2 TOF at $P_{CO}^{(n)} = 4.0 \times 10^{-10}$ atm. For example, the TOF of CO_2 is 1.9×10^{10} cm^{-2} s^{-1} at $P_{CO}^{(n)} = 3.0 \times 10^{-10}$ atm, which is about 200 times lower than the TOF of CO_2 at $P_{CO}^{(n)} = 4.0 \times 10^{-10}$ atm.

The CO oxidation activity changes dramatically as the $P_{CO}^{(n)}$ increases from 3.0×10^{-10} to 4.0×10^{-10} atm. This is due to the fact that the catalyst surface shifts from the oxygen-rich phase at $P_{CO}^{(n)} = 3.0 \times 10^{-10}$ atm to the CO-rich phase at $P_{CO}^{(n)} = 4.0 \times 10^{-10}$ atm. As shown in Fig. 3, the CO* surface coverage increases from 0.038 to 0.758 ML while the O* coverage decreases from 0.958 to 0.224 ML. Herein one monolayer surface coverage (1 ML) is defined as each surface site is occupied by one CO molecule or atomic O* atom. Therefore, the higher activity of CO oxidation is found when the RuO_2(1 1 0) surface is dominated by the adsorbed CO* molecules. This is consistent with the previous KMC simulation results [12,20]. As the $P_{CO}^{(n)}$ increases from 4.0×10^{-10} to 1.2×10^{-9} atm, the CO* coverage continues to increase to 0.981 ML while the O* coverage decreases to 0.014 ML. Although the surface phase is still the CO-rich surface phase, the total surface coverage actually slightly increases from 0.982 to 0.994 ML. As a result, CO oxidation activity is limited by the availability of active surface sites on the catalyst. As shown in Fig. 2, the CO_2 TOF gradually decreases as the $P_{CO}^{(n)}$ surpasses the optimum value of 4.0×10^{-10} atm.

The effects of heat and mass transfer on the CO oxidation kinetics are investigated by varying the thickness (d_z) of the RuO_2(1 1 0) surface slab. CO oxidation on a series of the RuO_2(1 1 0) surface slabs ranging from single layer ($d_z = 1$) to ten layers ($d_z = 10$) are studied as a function of $P_{CO}^{(n)}$ at $T^{(n)} = 350$ K and $P_{O_2}^{(n)} = 1.0 \times 10^{-10}$ atm. The simulated CO_2 TOFs shown in Fig. 2 clearly indicate that the reaction kinetics of CO oxidation pronouncedly depend upon the catalyst thickness at the same nominal reaction conditions. For the single layered RuO_2(1 1 0) catalyst, the TOF of CO_2 monotonically increases with the partial pressure $P_{CO}^{(n)}$. While for the RuO_2(1 1 0) catalyst with $d_z = 10$, the simulated TOF of CO_2 is close to the intrinsic TOF obtained from the pure KMC simulation without heat and mass transfer. The most active reaction condition with respect to the CO partial pressure on the RuO_2(1 1 0) catalyst with $d_z = 10$ is also found at $P_{CO}^{(n)} = 4.0 \times 10^{-10}$ atm although the simulated TOF of CO_2 is calculated as of 8.52×10^{12} cm^{-2} s^{-1}, which is two times higher than the intrinsic value at the same reaction condition. Furthermore, our simulation results indicate that the most active reaction condition shifts to the higher CO partial pressures as the RuO_2(1 1 0) catalyst becomes thinner. For example, as the thickness changes from $d_z = 10$ to $d_z = 3$, the most active reaction condition shifts from $P_{CO}^{(n)} = 4.0 \times 10^{-10}$ atm to $P_{CO}^{(n)} = 7.0 \times 10^{-10}$ atm.

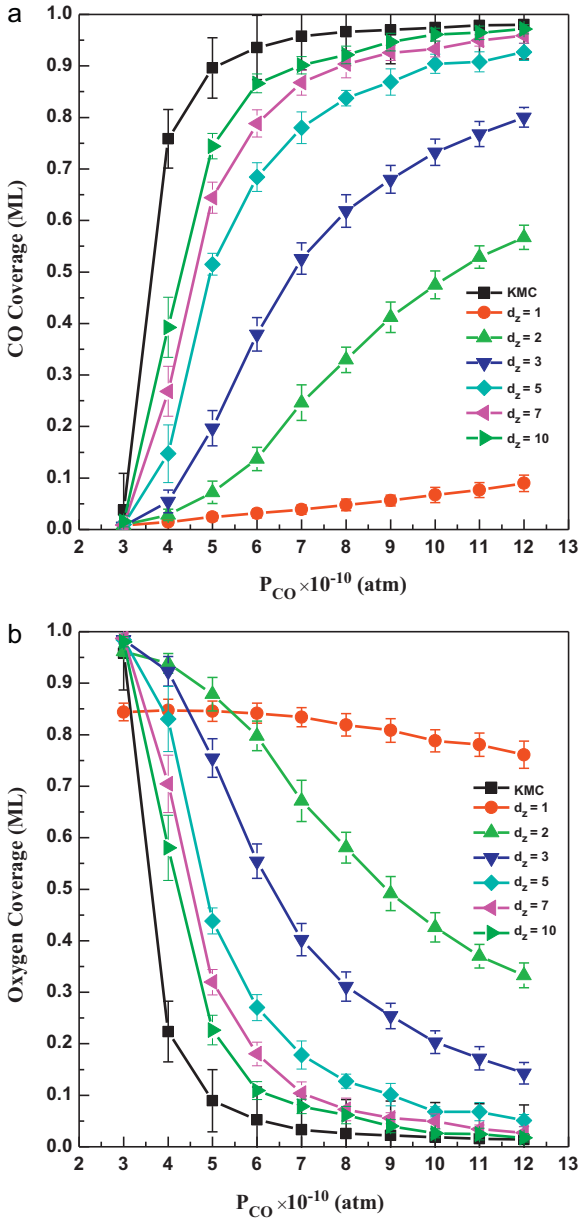

Fig. 3. Surface coverages as a fucntion of $P_{CO}^{(n)}$ at the nominal reaction condition of $T^{(n)} = 350$ K and $P_{O_2}^{(n)} = 1.0 \times 10^{-10}$ atm. (a) CO and (b) oxygen.

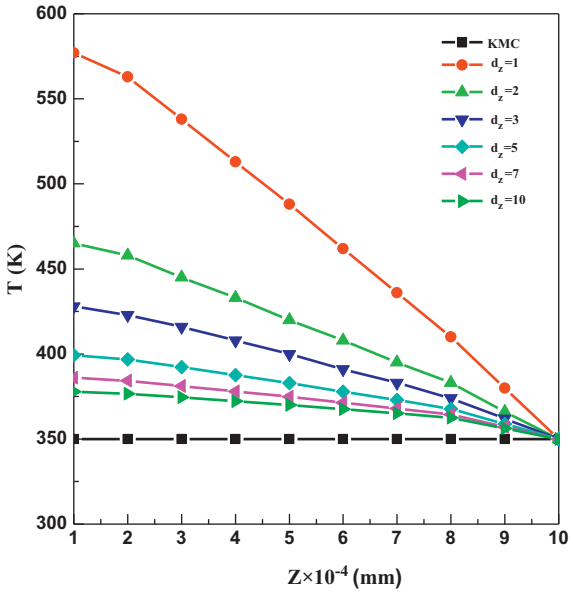

Fig. 4. Temperature gradient profiles in the boundary layer at the nominal reaction condition of $T^{(n)} = 350$ K, $P_{O_2}^{(n)} = 1.0 \times 10^{-10}$ atm and $P_{CO}^{(n)} = 4.0 \times 10^{-10}$ atm.

The simulated TOFs of CO_2 are higher than the intrinsic values obtained from pure KMC simulations at the same nominal reaction conditions. This is because the higher surface temperatures are obtained when the effect of heat transfer is considered. Since CO oxidation on the RuO_2(1 1 0) catalyst is exothermic and the reaction heat is not immediately removed from the system like the case of pure KMC simulations. As a result, the occurring CO oxidation tends to heat the catalyst. The increasing surface temperature further speeds up CO oxidation reaction rate, thus drives to a higher catalyst surface temperature. In the extreme condition, the surface temperature is so high that the catalyst surface reaches the uncontrollable condition of thermal runaway. Fig. 4 shows the simulated temperature gradients in the gas-phase boundary layer at nominal $T^{(n)} = 350$ K and partial pressures of $P_{CO}^{(n)} = 4.0 \times 10^{-10}$ atm and $P_{O_2}^{(n)} = 1.0 \times 10^{-10}$ atm. Again due to the exothermic nature of CO oxidation on the RuO_2(1 1 0) catalyst, the simulated surface temperatures are higher than the nominal temperature ($T^{(n)}$). The thinner the catalyst is, the higher surface temperature would be.

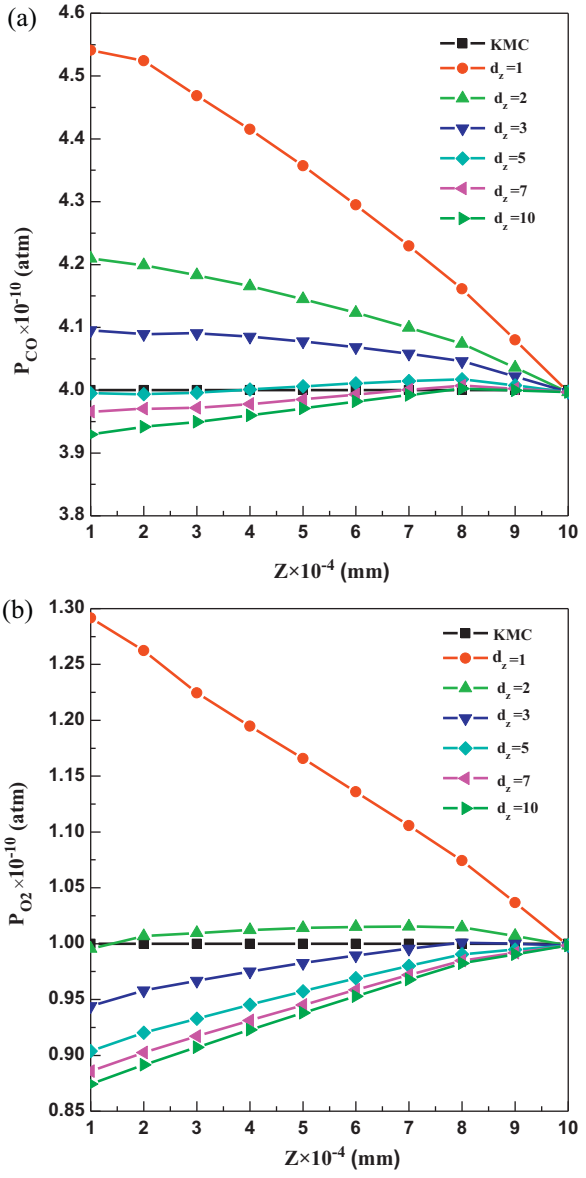

Fig. 5. Pressure gradient profiles in the boundary layer at the nominal reaction condition of $T^{(n)} = 350$ K, $P_{O_2}^{(n)} = 1.0 \times 10^{-10}$ atm and $P_{CO}^{(n)} = 4.0 \times 10^{-10}$ atm. (a) CO and (b) O_2.

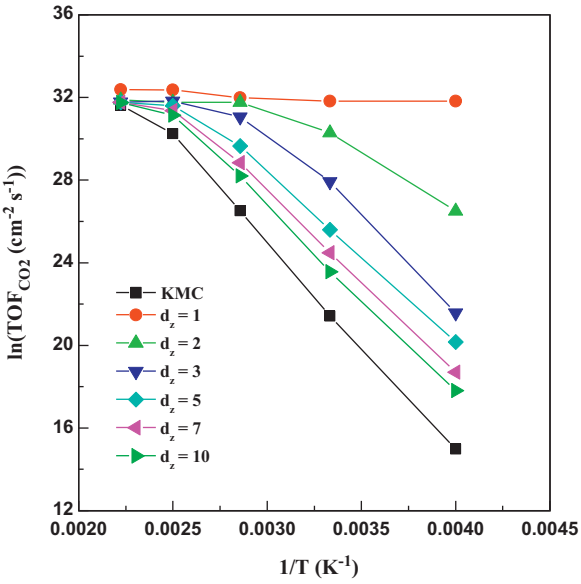

Fig. 6. Temperature dependence of the CO_2 TOFs at the nominal reaction condition of $P_{O_2}^{(n)} = 1.0 \times 10^{-10}$ atm and $P_{CO}^{(n)} = 4.0 \times 10^{-10}$ atm.

For the RuO_2(1 1 0) catalyst with $d_z = 10$, the surface temperature at the steady-state condition is 377 K, which is 27 K higher than the nominal temperature $T^{(n)}$. Bearing this in mind, it is not surprised that the TOFs of CO_2 is two times higher than the intrinsic value from the pure KMC simulation. For the single layered RuO_2(1 1 0) catalyst, the simulated surface temperature reaches at 577 K, which is 227 K higher than the temperature in the bulk gas-phase.

The temperature gradients in the gas-phase boundary layer is accompanying with the pressure gradients via mass transfer. The partial pressures in the adjacent gas-phase ($P_{CO}^{(1)}$ and $P_{O_2}^{(1)}$) above the catalyst surface are different from the nominal partial pressures ($P_{CO}^{(n)} = 4.0 \times 10^{-10}$ atm and $P_{O_2}^{(n)} = 1.0 \times 10^{-10}$ atm) in the bulk gas-phase. As shown in Fig. 5, the simulated $P_{CO}^{(1)}$ and $P_{O_2}^{(1)}$ for the RuO_2(1 1 0) catalyst with $d_z = 10$ are 3.93×10^{-10} and 8.70×10^{-11} atm, respectively. This indicates that the actual partial pressures imposed on the thicker catalysts are lower than the nominal partial pressures. Unlike the temperature gradients in the gas-phase boundary layer in which the surface temperatures are always higher than the temperatures in the bulk gas-phase, our simulation results show that the $P_{CO}^{(1)}$ and $P_{O_2}^{(1)}$ are higher than the $P_{CO}^{(n)}$ and $P_{O_2}^{(n)}$ for the thinner RuO_2(1 1 0) catalysts ($d_z < 3$). For example, the simulated $P_{CO}^{(1)}$ and $P_{O_2}^{(1)}$ are 4.54×10^{-10} and 1.29×10^{-10} atm for the single layered RuO_2(1 1 0) catalyst. This is because the temperatures of the gas-phase region that is adjacent to the catalyst surface are much higher than the nominal temperature in the bulk gas-phase.

Our simulations results are qualitatively consistent with the previous computational results by Matera and Reuter who also studied the effects of heat transfer on the CO_2 TOF under adiabatic heat conditions [13,14]. Under adiabatic heat limitation, the surface reaction heat is only allowed to be dissipated through the surrounding gas phase. As a result, their simulation results showed that the actual surface temperature is dramatically increased, resulting in very high reaction rates. They found that the surface temperature is about 150 K higher than the nominal reaction temperature, and the intrinsic activity of CO_2 is peaked at the stoichiometric partial pressure ratio. They concluded that the net effects of the surface temperature changes resulting from the transport limitation in the

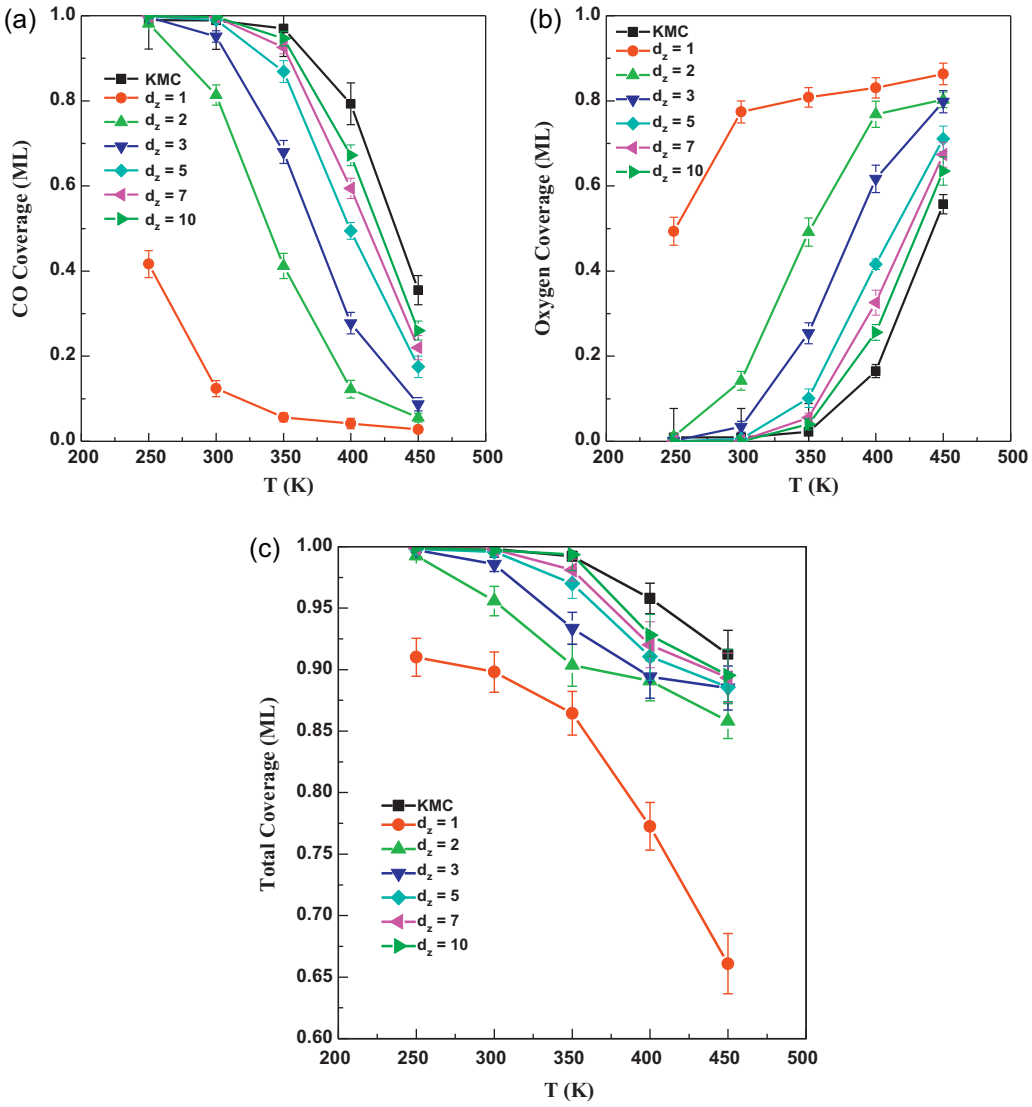

Fig. 7. Temperature dependence of the surface coverages at the nominal reaction condition of $P_{O_2}^{(n)} = 1.0 \times 10^{-10}$ atm and $P_{CO}^{(n)} = 4.0 \times 10^{-10}$ atm. (a) CO; (b) oxygen; (c) total coverage.

gas phase would substantially mask the intrinsic catalytic activity observed in the experiments [13,14]. We demonstrated the same effects in this work.

The apparent activation energy is one of the most important kinetics parameters for the heterogeneous reaction. To study the effect of the catalyst thickness on the apparent activation energy of CO oxidation on the RuO_2(1 1 0) catalyst, a series of simulations with different catalyst thicknesses in the temperature range of $T^{(n)}$ = 200–450 K at nominal partial pressures of $P_{CO}^{(n)} = 4.0 \times 10^{-10}$ and $P_{O_2}^{(n)} = 1.0 \times 10^{-10}$ atm have been performed. Using the classical Arrhenius relationship, the apparent activation energies of CO oxidation on the RuO_2(1 1 0) catalysts are obtained by the slope of logarithm of CO_2 TOF as the function of the inverse of temperature. Fig. 6 shows the apparent activation energies vary with the thickness of the RuO_2(1 1 0) catalyst. Without heat and mass transfer being considered in the gas-phase, the apparent activation energy calculated from the pure KMC simulations is 80.4 kJ/mol. By taking the effects of heat and mass transfer into account, the corresponding apparent activation energies at the same nominal reaction conditions become smaller. The apparent activation energies significantly decreases from 68.3 kJ/mol for the RuO_2(1 1 0) catalyst with d_z = 10 to 2.9 kJ/mol for the single layered RuO_2(1 1 0) catalyst. The smaller apparent activation energies for the thinner RuO_2(1 1 0) catalysts can be rationalized by the changes of the surface coverages of CO* and atomic O*. As the nominal reaction temperature ($T^{(n)}$) increases, the CO* coverage decreases (Fig. 7a) while the O* coverage increases (Fig. 7b) for all the catalysts with different thicknesses. We note the total surface overages on the thinner catalysts decrease much faster with the increasing nominal reaction temperature. This is consistent with our previous results that much higher surface temperatures are obtained for the thinner catalysts. As shown in Fig. 7c, the total coverage on the RuO_2(1 1 0) catalyst with d_z = 10 decreases from 0.999 to 0.260 ML as the $T^{(n)}$ increases from 250 to 450 K. The total coverage on the RuO_2(1 1 0) catalyst with d_z = 3, however, decreases from 0.996 to 0.087 ML in the same temperature range.

4. Conclusions

In this work, we proposed a heterogeneous reaction model that directly couples first-principles KMC simulation with a simple continuum model. The limitations of heat and mass transfer in the gas-phase boundary layer above the catalyst surface incur an actual reaction environment, which is different from the nominal

reaction conditions in the bulk gas-phase, for heterogeneous reaction. Using CO oxidation on the $RuO_2(1\,1\,0)$ catalyst as a testing system, we illustrated the macroscopic reaction kinetics of CO oxidation is dramatically affected by the thickness of the $RuO_2(1\,1\,0)$ catalyst. For the thinnest single layered $RuO_2(1\,1\,0)$ catalyst, the simulated apparent activation barrier is only 2.9 kJ/mol. This is due to the fact that the temperature of the gas-phase region that is directly imposed on the catalyst surface is much higher than the nominal temperature in the bulk gas-phase we presumed. Accompanying the temperature gradient, the significant pressure difference between the nominal values and the actual pressures on the catalyst also exists in the gas-phase boundary layer. With increasing thickness of the $RuO_2(1\,1\,0)$ catalyst, both temperature and pressure gradients alleviate. Although some assumptions had been made to simplify this hybrid simulation model, our results indicate that the observed reaction kinetics largely depends upon how the reaction heat, the reactants and products being exchanged with the invariant bulk gas-phase far from the surface. Even without including the bulk flow and the gas phase reactions, it is expected that the heat and mass transfer induced by the size and the heat conductivity properties of a catalyst could be the important factors in obtaining the intrinsic reaction kinetics in the experiments. To develop an accurate and reliable computational model for the heterogeneous reaction system, the limitations of heat and mass transfer in the surrounding reaction environment and their effects on the reaction kinetics are needed to be considered and included.

Acknowledgements

This work was financially supported by the Laboratory Directed Research and Development (LDRD) project at Pacific Northwest National Laboratory (PNNL) and Applied Mathematics program of the US DOE Office of Advanced Scientific Computing Research. The computing time was granted by the National Energy Research Scientific Computing Center at Lawrence Berkeley National Laboratory and the computational catalyst design project at the William R. Wiley Environmental Molecular Sciences Laboratory (EMSL). EMSL is a DOE national scientific user facility located at PNNL. D. Mei also acknowledged Prof. Karsten Reuter and Sebastian Matera for valuable discussions on the coupling issue, and for providing DFT parameters of CO oxidation on $RuO_2(1\,1\,0)$ used in this work. PNNL is operated by Battelle for the U.S. Department of Energy under Contract DE-AC05-76RL01830.

References

[1] M.P. Dudukovic, Science 325 (2009) 698.
[2] M.P. Dudukovic, Chem. Eng. Sci. 65 (2010) 3.
[3] A. Chatterjee, M.A. Snyder, D.G. Vlachos, Chem. Eng. Sci. 59 (2004) 5559.
[4] A. Chatterjee, D.G. Vlachos, Chem. Eng. Sci. 62 (2007) 4852.
[5] D.G. Vlachos, AIChE J. 43 (1997) 3031.
[6] D.G. Vlachos, A.B. Mhadeshwar, N.S. Kaisare, Comput. Chem. Eng. 30 (2006) 1712.
[7] A.B. Mhadeshwar, D.G. Vlachos, J. Phys. Chem. B 109 (2005) 16819.
[8] A.B. Mhadeshwar, D.G. Vlachos, J. Catal. 234 (2005) 48.
[9] V. Prasad, D.G. Vlachos, Ind. Eng. Chem. Res. 47 (2008) 6555.
[10] D. Majumder, L.J. Broadbelt, AIChE J. 52 (2006) 4214.
[11] A.B. Mhadeshwar, D.G. Vlachos, Ind. Eng. Chem. Res. 46 (2007) 5310.
[12] K. Reuter, M. Scheffler, Phys. Rev. B 73 (2006).
[13] S. Matera, K. Reuter, Catal. Lett. 133 (2009) 156.
[14] S. Matera, K. Reuter, Phys. Rev. B 82 (2010) 085446.
[15] D.W. Goodman, C.H.F. Peden, M.S. Chen, Surf. Sci. 601 (2007) L124.
[16] H. Over, Y.D. Kim, A.P. Seitsonen, S. Wendt, E. Lundgren, M. Schmid, P. Varga, A. Morgante, G. Ertl, Science 287 (2000) 1474.
[17] H. Over, M. Muhler, Prog. Surf. Sci. 72 (2003) 3.
[18] C.H.F. Peden, D.W. Goodman, J. Phys. Chem. 90 (1986) 1360.
[19] J. Wang, C.Y. Fan, K. Jacobi, G. Ertl, J. Phys. Chem. B 106 (2002) 3422.
[20] B. Temel, H. Meskine, K. Reuter, M. Scheffler, H. Metiu, J. Chem. Phys. 126 (2007) 204711.
[21] M. Neurock, D.H. Mei, Top. Catal. 20 (2002) 5.
[22] D.H. Mei, E.W. Hansen, M. Neurock, J. Phys. Chem. B 107 (2003) 798.
[23] D.H. Mei, Q.F. Ge, M. Neurock, L. Kieken, J. Lerou, Mol. Phys. 102 (2004) 361.
[24] L.D. Kieken, M. Neurock, D.H. Mei, J. Phys. Chem. B 109 (2005) 2234.
[25] D. Mei, P.A. Sheth, M. Neurock, C.M. Smith, J. Catal. 242 (2006) 1.
[26] D.H. Mei, M. Neurock, C.M. Smith, J. Catal. 268 (2009) 181.
[27] H. Meskine, S. Matera, M. Scheffler, K. Reuter, H. Metiu, Surf. Sci. 603 (2009) 1724.
[28] J. Crank, P. Nicolson, Math. Proc. Camb. Phil. Soc. 43 (1947) 50.
[29] S. Raimondeau, D.G. Vlachos, Chem. Eng. J. 90 (2002) 3.